MOLECULAR IMAGING AND BIOLOGY

Published Online: 11 August 2010

Mol Imaging Biol (2011) 13:769–775
DOI: 10.1007/s11307-010-0396-8

RESEARCH ARTICLE

^{68}Ga-DOTA-TATE PET vs. ^{123}I-MIBG in Identifying Malignant Neural Crest Tumours

Meeran Naji,[1] Chunlei Zhao,[2] Sarah J. Welsh,[1] Richard Meades,[1] Zarni Win,[1] Annalisa Ferrarese,[3] Tricia Tan,[4] Domenico Rubello,[5] Adil Al-Nahhas[1]

[1]*Department of Nuclear Medicine, Imperial College Healthcare Trust, London, UK*
[2]*Department of Nuclear Medicine, Second Affiliated Hospital of Zhejiang University School of Medicine, Hangzhou, China*
[3]*Service of Clinical Pharmacy, 'Santa Maria della Misericordia' Hospital, Rovigo, Italy*
[4]*Department of Endocrinology, Imperial College Healthcare Trust, London, UK*
[5]*Department of Nuclear Medicine, PET/CT Centre, Radiology, Medical Physics, Santa Maria della Misericordia' Hospital, Via Tre Martiri 140, 45100 Rovigo, Italy*

Abstract

Purpose: We aimed to compare imaging with ^{123}I-MIBG and ^{68}Ga-DOTA-TATE in neural crest tumours (NCT) to see if the latter could offer more advantage in detecting extra lesions and have higher sensitivity for malignant lesions.

Procedures: We retrospectively reviewed 12 patients (M=10, F=2; age range 20–71 years) with NCT (phaeochromocytomas = 7, paragangliomas = 4, medullary thyroid cancer = 1) who underwent both ^{68}Ga-DOTA-TATE positron emission tomography (PET) or PET/computed tomography (CT) and ^{123}I-MIBG single-photon emission computed tomography within 6 months. Visual assessment of all lesions and measurement of target/non-target (*T*/*N*) ratio in selected lesions were performed. Five patients (aged 50 or less) had SDHB screening results correlated with imaging results of both radiopharmaceuticals. All patients had contrast-enhanced CT and/or other cross-sectional imaging.

Results: ^{68}Ga-DOTA-TATE PET showed tumour lesions in ten out of 12 patients with confirmed disease, while ^{123}I-MIBG showed lesions in five out of 12 patients. In one patient, both ^{68}Ga-DOTA-TATE PET and ^{123}I-MIBG were negative, but CT, magnetic resonance imaging, and 2-deoxy-2-[^{18}F] fluoro-D-glucose PET scans identified a lesion in the thorax. ^{68}Ga-DOTA-TATE and ^{123}I-MIBG detected a total of 30 lesions, of which 29/30 were positive with ^{68}Ga-DOTA-TATE and 7/30 with ^{123}I-MIBG. We also found higher incidence of SDHB positive results in patients with positive ^{68}Ga-DOTA-TATE.

Conclusion: Our limited data suggest that ^{68}Ga-DOTA-TATE is a better imaging agent for NCT and detects significantly more lesions with higher *T*/*N* ratio compared to ^{123}I-MIBG. ^{68}Ga-DOTA-TATE was more likely to detect malignant lesions as indicated by correlating imaging results with SDHB screening.

Key words: ^{68}Ga-DOTA-TATE PET, ^{123}I-MIBG scintigraphy, Malignant neural crest tumours

Significance: The data of the present study are consistent with a higher sensitivity of Ga-DOTA-TATE PET in comparison with 123-MIBG conventional scintigraphy in detecting tumoral deposits of metastatic malignant neural crest tumours. This may be related both to the higher spatial resolution of the PET system in comparison with conventional gamma camera imaging and to the investigation of a different metabolic pathway of these tumours: the somatostatin receptor density evaluated by Ga68-DOTA-TATE in comparison with the catechomaminergic behaviour of the tumoral cells evaluated by 123-MIBS scintigraphy.

Correspondence to: Domenico Rubello; *e-mail:* domenico.rubello@libero.it

Introduction

Tumours of the neural crest are rare and have a wide range of clinical presentation and fascinating genetic association. Phaeochromocytoma is a good model of neural crest tumours (NCT) and may occur in association with hereditary syndromes including multiple endocrine neoplasia type 2A and 2B and Von Hippel Lindau disease. It arises in the adrenal medulla in 90% of cases, while 10% are extra-

adrenal known as paragangliomas. Genetic investigations have shown an association between two succinate dehydrogenase genes (SDHB & SDHD) and head and neck paragangliomas [1] which are more often malignant (15–35%) than phaeochromocytomas (10%) and may metastasize to bone, regional lymph nodes, liver, lung, and the brain [2].

The diagnosis of NCT is commonly done using a combination of cross-sectional imaging such as magnetic resonance imaging (MRI) and computed tomography (CT), and functional imaging, commonly ^{123}I-MIBG. The latter is reported to have less sensitivity (77–90%) than CT or MRI but higher specificity (>95%) [3]. However, concern has been raised regarding the use of MIBG as a screening tool since extra-adrenal disease and malignant lesions have been shown to have reduced affinity for MIBG [4]. Indium-111-octreotide may offer additional sensitivity [5], but the spatial resolution of single-photon emission computed tomography (SPECT) is inherently limited.

The recent introduction of positron emission tomography (PET) combined with CT (PET/CT) into clinical practise and the development of new PET radiopharmaceuticals have shown promising results in the detection of these tumours. ^{68}Ga-DOTA-TATE is a new high-affinity somatostatin receptor imaging agent that has shown higher detection rates in primary and metastatic phaeochromocytoma compared to ^{123}I-MIBG imaging [4]. It offers an additional advantage, i.e., the identification of patients likely to benefit from therapy with ^{90}Y-labelled DOTA-TATE [4, 6, 7].

The aim of this study was to evaluate the performance of ^{123}I-MIBG and ^{68}Ga-DOTA-TATE in the detection of NCT. Sensitivities of ^{123}I-MIBG and ^{68}Ga-DOTA-TATE were retrospectively assessed in 12 patients with NCT by measuring both the number of lesions and the maximum signal intensities compared to background obtained using each modality. To assess whether ^{68}Ga-DOTA-TATE is more sensitive in lesions with higher malignant potential, correlation with SDHB (as a mark of malignancy) was performed in patients below the age of 50 years.

Materials and Methods

Patients

We retrospectively reviewed 12 patients (M=10, F=2; age range 20–71 years) who underwent both ^{68}Ga-DOTA-TATE PET and ^{123}I-MIBG SPECT examinations between April 2005 and November 2009 at Imperial College Healthcare Trust. Among them, eight patients had histologically confirmed NCT (three phaeochrmocyomas, four paragangliomas, and one medullary thyroid cancer) and four patients had phaeochromocytoma or metastasis detected with cross-sectional imaging. All examinations took place within 6 months from each other (range 8–180 days, median 55 days) with no therapeutic interventions between the two examinations.

Imaging Techniques

CT Technique Helical CT of the neck, chest, abdomen and pelvis was performed using the LightSpeed Ultra CT scanner (General Electric Medical Systems, Milwaukee, Wisconsin, USA) with a collimation of 1.25 mm, a pitch of 1.5, and reconstructed using 3 mm slice thickness in the neck and 5 mm through the chest and abdomen. A bolus injection of 100 mL of 300 mg/mL non-ionic iodinated contrast medium was administered intravenously via a peripheral cannula at 3 mL/s by an injection pump. Blinded analysis of the CT images was performed by two radiologists on a PACS terminal (GE Healthcare Diagnostic Imaging, Slough, Berkshire, UK) and dedicated CT workstation. The site of the lesions and enhancement characteristics were documented by the readers in determining the nature of the lesion.

^{123}I-MIBG Technique ^{123}I-MIBG imaging was performed with a Siemens ECAM dual-headed gamma camera (Siemens, Hofmann Estates, Illinois, USA) after intravenous administration of 370-MBq (10 mCi) ^{123}I-MIBG (Tyco Healthcare (Mallinckrodt), Gosport, UK). Standard whole-body (simultaneous anterior and posterior views, 256×1,024 matrix, 10 cm/min, auto-contour) and SPECT acquisitions (128×128 matrix, 64 steps, 20 s per step, zoom 1.0, step-and-shoot mode over 360° non-circular orbit) were performed at 4 h and 24 h. Images were reconstructed using filtered back-projection algorithm (Butterworth filter, cutoff 0.5 Nyquist, order 5). A static posterior ^{123}I-MIBG image (128×128 matrix, zoom 1.0, 600 s) centred on the kidneys was also acquired at 24 h. This was combined with a static ^{99m}Tc-MAG3 image (100 MBq intravenous bolus injection, 128×128 matrix; zoom 1.0; dynamic acquisition, three phases of 40×1 s, 20×10 s and 11×60 s frames, summed to form a single image) to allow for masking of physiological uptake in the kidneys.

PET and PET/CT Technique PET imaging was performed using one of two scanners. In seven patients, scans were performed using a dedicated partial ring Siemens ART scanner (Siemens, Hamburg, Germany). Depending on the weight of the patients, 100–200 MBq (mean 150 MBq) of ^{68}Ga-DOTA-TATE [Tyco Healthcare (Mallinckrodt), Gosport, UK] was administered intravenously. Image acquisition was performed at 30-min post-injection, and patients were asked to empty their bladder. Half-body acquisitions were made from neck to pelvis. The acquisition time for each bed position was 12 min, consisting of emission scans in the 3-dimensional mode for 8-min and 4-min transmission scans using Cesium-137 sources for attenuation correction. Image reconstruction was performed using ordered subsets expectation maximisation algorithm (two iterations and 21 subsets).

The other five patients were scanned using Biograph TruePoint 64 PET CT (64 slice CT) System (Siemens, Hamburg, Germany). The CT exposure factors for all examinations were 50 mAs, 120 kV, 0.5 s/rot, pitch of 0.8 and slice thickness of 5 mm. Maintaining patient position, a whole-body PET scan was performed and covered an area identical to that covered by CT. PET acquisition was carried out in 3D with 2 min per bed position. PET images were reconstructed using CT for attenuation correction. Transaxial PET data were reconstructed using ordered subsets expectation maximisation algorithm (four iterations and eight subsets).

Histology

The histological findings were reviewed for all patients who underwent surgery by searching the clinical database used at Hammersmith Hospital (ICE System, Sunquest Systems Ltd, London, UK).

SDHB Status

Patients below the age of 50 years were screened for SDHB mutations, and the results were correlated with the findings of the ^{68}Ga-DOTA-TATE and ^{123}I-MIBG scans.

Data Analysis

All scintigraphic images were reviewed on a Hermes workstation (Nuclear Diagnostics, Sweden) by two experienced nuclear medicine physicians. Areas of increased non-physiologic uptake in either planar or tomographic images were defined as positive lesions with the consensus of the two physicians.

The site and number of lesions were assessed. The lesions seen in each study underwent further evaluation to compare the intensity of the uptake for lesions. The standard uptake value (SUV) was not available for either ^{68}Ga- DOTA-TATE (due to calibration issues) or ^{123}I-MIBG SPECT. Since the SUV used in PET imaging was not available for ^{123}I-MIBG SPECT, we introduced a quantitative parameter of target to non-target (*T*/*N*) ratio which was calculated based on analysis of counts in regions of interest (ROI). For each lesion, ROI were drawn around the lesion on all axial images containing it, and the maximum pixel count was recorded. Then, a background (BK) ROI was drawn in the lung fields, and the mean pixel count was recorded. All drawing conditions for ROI analysis were kept the same. *T*/*N* ratio was then calculated using following equation:

$$T/N \text{ ratio} = \text{maximum count for lesion/mean count in BK ROI}$$

Results

Analysis on Patient Basis

^{68}Ga-DOTA-TATE PET showed tumour lesions in ten out of 12 patients with confirmed disease. However, of the two patients in which ^{68}Ga-DOTA-TATE PET failed to detect tumour, ^{123}I-MIBG detected disease in one patient. On the other hand, ^{123}I-MIBG showed lesions in five out of 12 patients with confirmed disease, but failed to detect tumour in seven patients. Of the seven patients, ^{68}Ga-DOTA-TATE PET detected disease in six (Tables 1 & 2). The sensitivity of ^{68}Ga-DOTA-TATE PET was 83% (10/12), of ^{123}I-MIBG, was 42 (5/12), and for combined ^{68}Ga-DOTA-TATE and ^{123}I-MIBG, was 92% (11/12). In one patient, both ^{68}Ga-DOTA-TATE PET and ^{123}I-MIBG were negative, but CT, MRI and 2-deoxy-2-[^{18}F]fluoro-D-glucose ([^{18}F]FDG) PET scans identified a lesion in the right hilum.

Table 1. Comparison of results of ^{123}I-MIBG and ^{68}Ga-DOTA-TATE scans

	Positive ^{123} I MIBG	Negative ^{123} I MIBG	Total
Positive ^{68}Ga DOTA-TATE	4	6	10
Negative ^{68}Ga DOTA-TATE	1	1	2
Total	5	7	12

Analysis on Lesion Basis

^{68}Ga-DOTA-TATE and ^{123}I-MIBG detected a total of 30 lesions of variable sizes ranging from 3 to 49 mm (mean 18 mm). Of those, 29/30 lesions were positive with ^{68}Ga-DOTA-TATE and 7/30 with ^{123}I-MIBG (Fig. 1). One lesion was negative on both the ^{68}Ga-DOTA-TATE and ^{123}I-MIBG scans, but positive on the CT, MRI and [^{18}F]FDG PET scans. Twenty-three lesions in eight patients were detected in ^{68}Ga-DOTA-TATE scans but not in ^{123}I-MIBG scans. One lesion in one patient was detected in ^{123}I-MIBG scan but not in ^{68}Ga-DOTA-TATE scan (Table 2).

For the quantitative comparison of the concordant lesions, *T*/*N* ratios in ^{68}Ga-DOTA-TATE scans were higher, ranging from 10.7 to 397 (mean 96) compared to those obtained with ^{123}I-MIBG scans (range 2.8–45 with a mean of 16.2).

Analysis on the Basis of SDHB

Five patients below the age of 50 years had SDHB screening tests (Table 2). Of those, the test was positive in four. Three patients with positive SDHB test had lesions detected with ^{68}Ga-DOTA-TATE but missed with ^{123}I-MIBG. One patient with positive SDHB test had negative ^{68}Ga-DOTA-TATE and ^{123}I-MIBG. The fifth patient with negative SDHB test had one lesion detected with ^{123}I-MIBG but not with ^{68}Ga-DOTA-TATE.

Discussion

NCT originate from the embryonic neural crest tissue which lies adjacent to the neural tube, and these include phaeochromocytoma, paraganglioma and medullary cell carcinoma of the thyroid gland [8]. The management of malignant NCT requires early detection and screening for mutations in the SDH enzyme subunits as these may point to a malignant potential.

SDH is an enzyme complex composed of four subunits encoded by four nuclear genes (SDHA, SDHB, SDHC and SDHD) [9]. It has an important function in the Krebs cycle and mitochondrial respiratory chain in a way that prevents the formation of potentially dangerous reactive oxygen species [10]. It has been recently noted that genetic variants and mutations in the SDHB, SDHC, and SDHD subunits are associated with hereditary phaeochromocytoma syndromes and malignant paraganglioma [11–13]. These mutations cause destabilisation of the SDH complex and activation of hypoxic pathways predisposing to tumour formation [14]. Recent studies showed that SDHB mutations are most

Table 2. Neural crest tumours—tracer uptake in ^{68}Ga-DOTA-TATE and ^{123}I-MIBG and correlation with SDHB mutation

Patient no.	Diagnosis	Confirmation	SDHB status	Lesions detected with ^{68}Ga DOTA-TATE	Lesions detected with ^{123}IMIBG	Size of lesions	Duration between scans (days)
1	Paraganglioma	Histology	Positive	Bone, 11, LN, 4	Bone, 3	15 lesions range from 3–28 mm (the largest five lesions in the spine range 19–28 mm)	25
2	Phaeochromocytoma	Histology	–	Adrenal, 1	Adrenal, 1	24 mm	70
3	Phaeochromocytoma	MRI	–	Adrenal, 1	Adrenal, 1	28 mm	25
4	Medullary thyroid Ca.	Histology	–	Bone, 1; mediastinum, 4	0	Range from 5 to 10 mm	150
5	Phaeochromocytoma	CT	Negative	0	Bone, 1	11 mm	45
6	Phaeochromocytoma	Histology	–	LN, 2	LN, 1	12 mm, 14 mm	89
7	Paraganglioma	Histology	Positive	0	0	–	22
8	Paraganglioma	Histology	Positive	Carotid/neck, 1	0	12 mm	88
9	Phaeochromocytoma	CT + FDG PET	–	Adrenal, 1	0	23 mm	81
10	Paraganglioma	Histology	Positive	Carotid/neck, 1	0	8 mm	8
11	Phaeochromocytoma	Histology	–	Adrenal, 1	0	49 mm	9
12	Phaeochromocytoma	CT	–	Adrenal, 1	0	18 mm	180

LN lymph nodes

frequently associated with extra-adrenal sympathetic paragangliomas [1, 15, 16], and these mutations are usually found in patients who present with the disease below the age of 50 years. In a study of 83 patients with phaeochromocytoma/paraganglioma who were older than 50 years at diagnosis, only one patient was found to have a gene mutation. The findings of this study support similar findings from other studies and suggest that genetic counselling and screening should only be offered to patients with phaeochromocytoma who are below the age 50 years [17].

Anatomical imaging with CT, MRI and ultrasound is extensively used for the detection of NCT [18]. CT has a high sensitivity of 93–100% for detecting adrenal phaeochromocytoma of approximately 0.5 cm in diameter [19]. However, the sensitivity drops to 90% for localising extra-adrenal disease [19]. In comparison, reports suggest that MRI has a slightly better sensitivity. It has been recommended that cross-sectional imaging with CT or MRI should be used in patients with biochemically proven phaeochromocytoma or paraganglioma. CT and MRI are found to be particularly useful when the biochemical tests are negative as the likelihood of having phaeochromocytoma would be very low. However, the specificity of cross-sectional imaging ranges from 50% to 90% [19]. Thus, positive studies may not be diagnostic [20] particularly in patients with previous surgery. In these patients and in cases of extra-adrenal, malignant or metastatic disease, the use of functional imaging is usually advocated [19].

Fig. 1. Number of lesions visualised with ^{123}I-MIBG scintigraphy and/or ^{68}Ga-DOTA-TATE PET.

^{123}I-MIBG scintigraphy is one of the most widely used functional imaging modalities for the diagnosis and staging of NCT. Metaiodobenzylguanidine (MIBG) is a catecholamine precursor that has a mechanism of uptake and storage similar to norepinephrine. Once it enters the cells, MIBG is actively transported into the intracellular catecholamine-storing granules by means of an ATPase-dependent proton pump [21–23]. ^{123}I-MIBG is useful in localising phaeochromocytomas particularly those in areas of previous surgery where anatomical imaging may be compromised by distortion of anatomy and the presence of metallic clips that degrade CT and MRI images [24]. ^{123}I-MIBG scintigraphy has excellent specificity for detecting phaeochromocytoma; however, it has several disadvantages including reduced resolution and poor image quality resulting in limited sensitivity [25]. In addition, it requires a 2-day imaging protocol and a supplementary $^{99\,m}$Tc-MAG3 scan to identify the kidneys.

Somatostatin receptor imaging has been used in the investigation of suspected phaeochromocytoma and paraganglioma. ^{111}In-octreotide is a somatostatin analogue which targets somatostatin receptors (STR) that are over-expressed in NCT. The overall sensitivity of ^{111}In-octreotide in detecting NCT is relatively low when compared to ^{123}I-

MIBG, with the exception of patients with suspected head and neck paraganglioma [26]. In this group of patients, ^{111}In-octreotide scintigraphy is proven to be superior to ^{123}I-MIBG in detecting more lesions with better imaging properties. In a study of 29 patients with paraganglioma, Coopmans *et al*. showed that both ^{111}In-octreotide and cross-sectional imaging were positive in 27 patients (sensitivity 93%), whereas ^{123}I-MIBG was positive in 13 (sensitivity 44%), suggesting that ^{111}In-octreotide is probably the functional imaging agent of choice for the assessment of head and neck paraganglioma that can be useful when there is a high clinical suspicion with negative ^{123}I-MIBG scan [27]. However, the main disadvantage of ^{111}In-octreotide scintigraphy remains the inherent limited spatial resolution of SPECT.

With PET technology, functional imaging with higher spatial resolution than conventional scintigraphy can be obtained [28]. The most widely used PET tracer, [^{18}F]FDG, has been shown to be of great value in the detection of adrenal malignancies [29]. Several studies have evaluated the role of [^{18}F]FDG in imaging benign and malignant phaeochromocytomas and found that most of these tumours are metabolically active and could be localised with [^{18}F]FDG PET [24, 30]. Shulkin *et al*. detected phaeochromocytoma with [^{18}F]FDG PET in 22 of 29 patients (sensitivity 76%). Most pheochromocytomas (7/12 benign) and (15/17 malignant) avidly accumulated [^{18}F]FDG, although the uptake was found in a greater percentage in malignant than benign tumours [31]. Interestingly, some phaeochromocytomas with poor concentration of ^{123}I-MIBG were well detected with [^{18}F]FDG, while tumours which failed to accumulate [^{18}F]FDG were visualised better with ^{123}I-MIBG [32]. Based on this fact, recent studies suggest that [^{18}F]FDG PET may play a role in imaging patients with phaeochromocytoma that have negative ^{123}I-MIBG [31, 33] and patients with positive SDHB test (more prone to malignant disease) [28]. However, [^{18}F]FDG is a glucose analogue that tends to accumulate in a variety of neoplastic and non-neoplastic processes resulting in a low specificity. Therefore, [^{18}F]FDG PET cannot be recommended as first-line investigation of phaeochromocytoma and paraganglioma [29].

The diagnosis of NCT can also be made using other specific PET agents that target the catecholamine synthesis, transport and storage pathways. These include 6-18F-fluoro-L-3,4-dihydroxyphenylalanine (^{18}F-DOPA) and 6-18F-fluorodopamine (^{18}F-FDA). The dopamine precursor, ^{18}F-DOPA, was originally developed to image neurodegenerative disorders, but subsequent studies showed that it could also be used to image chromaffin tumours with high sensitivity and excellent specificity [26]. In a very recent study, Timmers *et al*. compared the sensitivity of ^{18}F-DOPA, ^{18}F-FDA, [^{18}F]FDG and ^{123}I-MIBG in 52 patients with phaeochromocytoma or paraganglioma. Interestingly, the study showed that non-metastatic paragangliomas were equally detected by these four techniques with sensitivities of 81% for ^{18}F-DOPA, 78% for ^{18}F-FDA, 88% for [^{18}F]FDG, and 78% for ^{123}I-MIBG, whereas, metastatic paragangliomas were best detected by ^{18}F-FDA with reported sensitivities of 76% for ^{18}F-FDA, 45% for ^{18}F-DOPA, 74% for [^{18}F]FDG, and 57% for ^{123}I-MIBG scintigraphy. In addition, the study revealed that ^{18}F-FDA and [^{18}F]FDG have a higher sensitivity (82% and 83%, respectively) for the localisation of SDHB-related metastatic disease compared to the sensitivity of ^{123}I-MIBG (57%) and ^{18}F-DOPA (20%) [34]. Despite these promising results, the limited availability remains the main disadvantage of these agents (^{18}F-DOPA and ^{18}F-DA) [26].

Another approach to image NCT is to use a PET tracer labelled to somatostatin analogues such as ^{68}Ga-DOTA-TATE, taking the advantage of STR that are over-expressed in these tumours [35]. Recent reports suggest that PET imaging with ^{68}Ga-DOTA-TATE may play a role in the management of NCT particularly in patients with malignant disease and those who have negative or very weakly positive ^{123}I-MIBG. In a recent study, Kayani I *et al*. evaluated the role of ^{68}Ga-DOTA-TATE in imaging neuroendocrine tumours (NET) in 38 patients and compared its performance with [^{18}F]FDG. The study revealed that ^{68}Ga-DOTA-TATE has a higher sensitivity of 82% for detecting NET compared to 66% for [^{18}F]FDG. Interestingly, there was greater uptake of ^{68}Ga-DOTA-TATE than [^{18}F]FDG in low-grade tumours, whereas in high-grade lesions, there was higher uptake of [^{18}F]FDG over ^{68}Ga-DOTA-TATE indicating that ^{68}Ga-DOTA-TATE and [^{18}F]FDG exploit different tumour characteristics, and these two tracers may play a complementary role in imaging patients with metastatic disease [36].

1^{68}Ga-DOTA-TATE has shown several advantages over other tracers. By targeting somatostatin receptors, it is more tumour-specific than [^{18}F]FDG, which is a glucose analogue relying on the non-specific glucose metabolism [4]. Compared to MIBG, ^{68}Ga-DOTA-TATE also has the inherent superiority of PET compared to SPECT. An additional advantage is the all year-round availability of in-house ^{68}Ge/^{68}Ga generator with daily supply for more than a year. In departments with heavy load of NET and NCT, this is an extremely cost-effective procedure negating the need for on-site cyclotron.

Our data demonstrate that ^{68}Ga-DOTA-TATE PET is superior to ^{123}I-MIBG in the detection of malignant NCT demonstrating more lesions with higher *T*/*N* uptake ratio. Figure 2 is an example of a patient with known recurrent paraganglioma who was shown to have vertebral metastases on CT (Fig. 2a). He had ^{123}I-MIBG scan, which showed three vertebral lesions with minimally increased uptake (Fig. 2b–c). His ^{68}Ga-DOTA-TATE PET CT revealed numerous vertebral lesions as well as multiple soft tissue and lymph nodes involvement (Fig. 2d).

In our study, 23 lesions were detected with ^{68}Ga-DOTA-TATE PET and missed with ^{123}I-MIBG compared to one lesion detected with ^{123}I-MIBG but missed with ^{68}Ga-DOTA-TATE PET. The size of lesions did not play a role in the superior detection of ^{68}Ga-DOTA-TATE since most

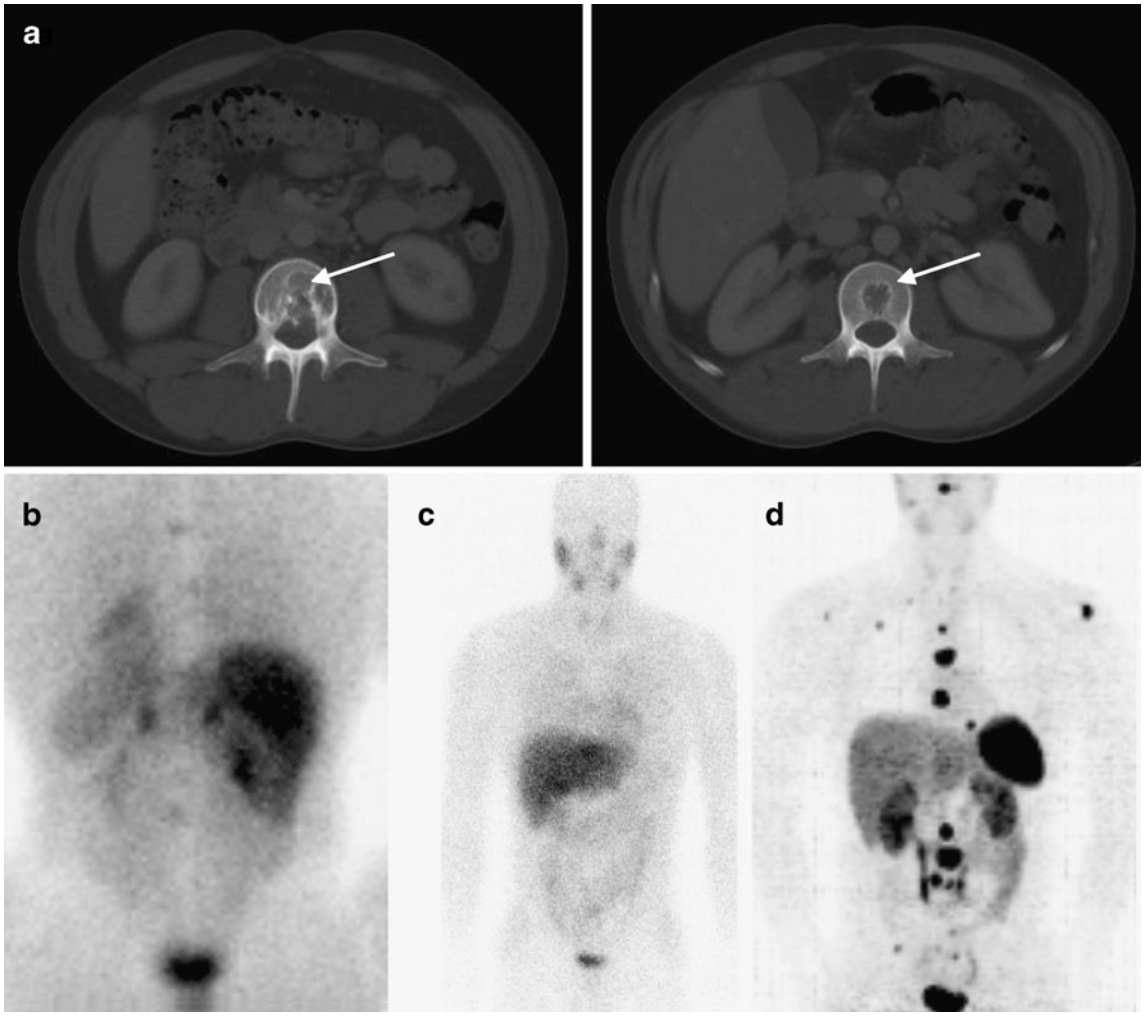

Fig. 2. Patient with paraganglioma and multiple bony and lymph node metastases. **a** Two axial CT images showing metastasis in lumbar vertebral bodies (*white arrows*), **b** posterior ^{123}I-MIBG scan showing minimally increased uptake in two lower dorsal and one lumbar vertebrae, **c** anterior ^{123}I-MIBG scan shown for anterior comparison with, **d** ^{68}Ga-DOTA-TATE maximum intensity image showing multiple vertebral lesions, as well as multiple soft tissue and lymph node metastases.

of the lesions that were detected with ^{68}Ga-DOTA-TATE but missed with ^{123}I-MIBG measured more than 10 mm (the largest 49 mm) well within the resolution of ^{123}I-MIBG. We also found that the physiological DOTA-TATE accumulation was low and *T/N* ratios were usually high. In addition, our study showed that patients with positive SDHB test had lesions detected with ^{68}Ga-DOTA-TATE but missed with ^{123}I-MIBG suggesting a possible link between positive SDHB mutation and tumour accumulation of ^{68}Ga-DOTA-TATE.

We recommend that initial localisation of phaeochromocytomas and paragangliomas be performed with cross-sectional imaging and MIBG scintigraphy. However, patients with negative MIBG scintigraphy, particularly when suspected of being malignant, should have further imaging with ^{68}Ga-DOTA-TATE PET, in view of the possible therapy with ^{90}Yttrium or ^{177}Lutetium-labelled DOTA-TATE.

Conclusion

Imaging with ^{68}Ga-DOTA-TATE PET is superior to ^{123}I-MIBG in the detection of malignant NCT demonstrating more lesions with higher tumour to background uptake ratio and better resolution. In addition, the findings of our study suggest a possible link between positive SDHB mutation and tumour accumulation of ^{68}Ga-DOTA-TATE. However, larger series are required to establish its clinical significance.

Conflict of Interest Statement. The authors declare they have no conflict of interest in the preparation of the present paper.

References

1. Neumann HP, Bausch B, McWhinny SR, Bender BU, Gimm O, Franke G et al (2002) Germ-line mutations in nonsyndromic pheochromocytoma. N Engl J Med 346:1459–1466

2. O'Riordain D, Young WF, Grant CS, Carney JA, van Heerden (1996) Clinical spectrum and outcome of functional extraadrenal paraganglioma. World J Surg 20:916–922
3. Reisch N, Peczkowska M, Januszewicz A, Neumann HP (2006) Pheochromocytoma: presentation, diagnosis and treatment. J Hypertens 24:2331–2339
4. Win Z, Al-Nahhas A, Towey D, Todd JF, Rubello D, Lewington V, Gishen P (2007) 68Ga-DOTATATE PET in neuroectodermal tumours: first experience. Nucl Med Commun 28:359–363
5. Ilias I, Chen CC, Carrasquillo JA, Whatley M, Ling A, Lazurova I et al (2008) Comparison of 6-18F-fluorodopamine positron emission tomography to 123I-metaiodobenzylguanidine and 111In-pentetreotide scintigraphy in the localization of non-metastatic and metastatic pheochromocytoma. J Nucl Med 49:1613–1619
6. Lewigton VJ (2003) Targeted radionuclide therapy for neuroendocrine tumours. Endocr-Relat Cancer 10:497–501
7. Kwekkeboom DJ, Mueller-Brand J, Paganelli G, Anthony LB, Pauwels S, Kvols LK et al (2005) Overview of results of peptide receptor radionuclide therapy with 3 radiolabeled somatostatin analogs. J Nucl Med 46(Suppl 1):62S–66S
8. Smith SL, Vincent RM, Perkins AC, Wastie ML, Sokal M (2001) Does simple estimation of ^{131}I-metaiodobenzylguanidine uptake in patients with neural crest tumours correlate with clinical outcome? Nucl Med Commun 22:257–260
9. Pasini B, Stratakis CA (2009) SDH mutations in tumorigenesis and inherited endocrine tumours: lesson from the phaeochromocytoma-paraganglioma syndromes. J Intern Med 266(1):19–42
10. Yankovskaya V, Horsefield R, Törnroth S, Luna-Chavez C, Miyoshi H, Léger C et al (2003) Architecture of succinate dehydrogenase and reactive oxygen species generation. Science 299:700–704
11. Astuti D, Latif F, Dallol A, Dahia PL, Douglas F, George E et al (2001) Gene mutations in the succinate dehydrogenase subunit SDHB cause susceptibility to familial pheochromocytoma and to familial paraganglioma. Am J Hum Genet 69:49–54
12. Baysal BE, Ferrell RE, Willett-Brozick JE, Lawrence EC, Myssiorek D, Bosch A et al (2000) Mutations in SDHD, a mitochondrial complex II gene, in hereditary paraganglioma. Science 287:848–851
13. Niemann S, Muller U (2000) Mutations in SDHC cause autosomal dominant paraganglioma, type 3. Nat Genet 26:268–270
14. Karagiannis A, Mikhailidis DP, Athyros VG, Harsoulis F (2007) Pheochromocytoma: an update on genetics and management. Endocr-Relat Cancer 14:935–956
15. Benn DE, Gimenez-Roqueplo A-P, Reilly JR, Bertherat J, Burgess J, Byth K et al (2006) Clinical presentation and penetrance of pheochromocytoma/paraganglioma syndromes. J Clin Endocrinol Metab 91:27–836
16. Klein RD, Jin L, Rumilla K, Young WF Jr, Lloyd RV (2008) Germline SDHB mutations are common in patients with apparently sporadic sympathetic paragangliomas. Diagn Mol Pathol 17(2):94–100
17. Bryant J, Farmer J, Kessler LJ, Townsend RR, Nathanson KL (2003) Pheochromocytoma: the expanding genetic differential diagnosis. J Natl Cancer Inst 95(16):1196–1204
18. Chrisoulidou A, Kaltsas G, Ilias I, Grossman AB (2007) The diagnosis and management of malignant phaeochromocytoma and paraganglioma. Endocr-Relat Cancer 14(3):569–585
19. Ilias I, Pacak K (2004) Current approaches and recommended algorithm for the diagnostic localization of pheochromocytoma. J Clin Endocrinol Metab 89:479–491
20. Go AS (1998) Refining probability: an introduction to the use of diagnostic tests. In: Friedland DJ (ed) Evidence-based medicine. McGraw-Hill, New York, pp 12–33
21. Wieland DM, Wu JL, Brown LE (1980) Radiolabelled adrenergic neuron blocking agents: adrenomedullary imaging with 131Iiodobenzylguanidine. J Nucl Med 21:349–353
22. Beierwaltes WH (1991) Endocrine imaging: parathyroid, adrenal cortex and medulla, and other endocrine tumors. Part II. J Nucl Med 32:1627–1639
23. McEwan AJ, Shapiro B, Sisson JC, Beierwaltes WH, Ackery DM (1985) Radioiodobezylguanidine for the scintigraphic location and therapy of adrenergic tumors. Semin Nucl Med 15:132–153
24. Shulkin BL, Ilias I, Sisson JC, Pacak K (2006) Current trends in functional imaging of pheochromocytomas and paragangliomas. Ann NY Acad Sci 1073:374–382
25. Mann GN, Link JM, Pham P, Pickett CA, Byrd DR, Kinahan PE et al (2006) 11C-metahydroxyephedrine and 18F-fluorodeoxyglucose positron emission tomography improve clinical decision making in suspected phaeochromocytoma. Ann Surg Oncol 13(2):187–197
26. Reynolds S, Lewington V (2008) Radionuclide imaging of phaeochromocytoma and paraganglioma. Imaging 34:21–24
27. Koopmans KP, Jager PL, Kema IP, Kerstens MN, Albersy F, Dullaart RPF (2008) ^{111}In-octreotide is superior to ^{123}I-metaiodobenzylguanidine for scintigraphic detection of head and neck paragangliomas. J Nucl Med 49:1232–1237
28. Ilias I, Pacak K (2008) A clinical overview of pheochromocytomas/paragangliomas and carcinoid tumors. Nucl Med Biol 35(Suppl 1):S27–S34
29. Brink I, Hoegerle S, Klisch J, Bley TA (2005) Imaging of pheochromocytoma and paraganglioma. Fam Cancer 4(1):61–68
30. Maurea S, Mainolfi C, Wang H, Varrella P, Panico MR, Klain M et al (1996) Positron emission tomography (PET) with fludeoxyglucose F 18 in the study of adrenal masses: comparison of benign and malignant lesions. Radiol Med 92:782–787
31. Shulkin BL, Thompson NW, Shapiro B, Francis IR, Sisson JC (1999) Pheochromocytomas: imaging with 2-[fluorine-18]fluoro-2-deoxy-D-glucose PET. Radiology 212:35–41
32. Neumann DR, Basile KE, Bravo EL, Chen EQ, Go RT (1996) Malignant phaeochromocytoma of the anterior mediastinum: PET findings with [18F] FDG and 82Rb. J Comput Assist Tomogr 20:312–316
33. Mamede M, Carrasquillo JA, Chen CC, Del Corral P, Whatley M, Ilias I et al (2006) Discordant localization of 2-[18F]-fluoro-2-deoxy-D-glucose in 6-[18F]-fluorodopamine- and [(123)I]-metaiodobenzylguanidine-negative metastatic pheochromocytoma sites. Nucl Med Commun 27:31–36
34. Timmers H, Chen C, Carrasquillo J, Whatley M, Ling A, Havekes B et al (2009) Comparison of 18F-fluoro-L-DOPA, ^{18}F-fluoro-deoxyglucose, and ^{18}F-fluorodopamine PET and ^{123}I-MIBG scintigraphy in the localization of pheochromocytoma and paraganglioma. J Clin Endocrinol Metab 94(12):4757–4767
35. Khan S, Lloyd C, Szyszko T, Win Z, Rubello D, Al-Nahhas A (2008) PET imaging in endocrine tumours. Minerva Endocrinol 33 (2):41–52
36. Al-Nahhas A, Win Z, Szyszko T, Singh A, Khan S, Rubello D (2007) What can gallium-68 PET add to receptor and molecular imaging? Eur J Nucl Med Mol Imaging 34(12):1897–1901